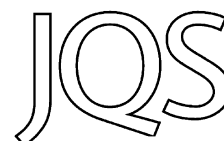


## Rapid Communication

# $^{36}\text{Cl}$ production rate from K-spallation in the European Alps (Chironico landslide, Switzerland)



IRENE SCHIMMELPFENNIG,<sup>1,2\*,†</sup> JOERG M. SCHAEFER,<sup>1</sup> AARON E. PUTNAM,<sup>1,3</sup>  
TOBY KOFFMAN,<sup>1,3</sup> LUCILLA BENEDETTI,<sup>2</sup> SUSAN IVY-OCHS,<sup>4</sup> ASTER TEAM<sup>2,‡</sup> and CHRISTIAN SCHLÜCHTER<sup>5</sup>

<sup>1</sup>Lamont-Doherty Earth Observatory, Columbia University, Palisades, NY, USA

<sup>2</sup>Aix-Marseille Université, CNRS-IRD, Collège de France, Aix-en-Provence, France

<sup>3</sup>Department of Earth Sciences and Climate Change Institute, University of Maine, Orono, ME, USA

<sup>4</sup>Institut für Teilchenphysik, Eidgenössische Technische Hochschule, Zürich, Switzerland

<sup>5</sup>Institute of Geological Sciences, University of Bern, Switzerland

Received 28 January 2014; Revised 18 April 2014; Accepted 12 May 2014

**ABSTRACT:** The abundant production of *in situ* cosmogenic  $^{36}\text{Cl}$  from potassium renders  $^{36}\text{Cl}$  measurements in K-rich rocks or minerals, such as K-feldspars, potentially useful for precisely dating rock surfaces, either in single-nuclide or in multi-nuclide studies, for example combined with  $^{10}\text{Be}$  measurements in quartz. However, significant discrepancies in experimentally calibrated  $^{36}\text{Cl}$  production rates from spallation of potassium ( $^{36}\text{P}_{\text{K-sp}}$ ), referenced to sea-level/high-latitude (SLHL), limit the accuracy of  $^{36}\text{Cl}$  dating from K-rich lithologies. We present a new  $^{36}\text{Cl}$  calibration using K-feldspars, in which K-spallation is the most dominant  $^{36}\text{Cl}$  production pathway (>92% of total  $^{36}\text{Cl}$ ), thus minimizing uncertainties from the complex multi-pathway  $^{36}\text{Cl}$  production systematics. The samples are derived from boulders of an ~13.4 ka-old landslide in the Swiss Alps (~820 m, 46.43°N, 8.85°E). We obtain a local  $^{36}\text{P}_{\text{K-sp}}$  of  $306 \pm 16$  atoms  $^{36}\text{Cl} (\text{gK})^{-1} \text{a}^{-1}$  and an SLHL  $^{36}\text{P}_{\text{K-sp}}$  of  $145.5 \pm 7.7$  atoms  $^{36}\text{Cl} (\text{gK})^{-1} \text{a}^{-1}$ , when scaled with a standard scaling protocol ('Lm'). Applying this SLHL  $^{36}\text{P}_{\text{K-sp}}$  to determine  $^{36}\text{Cl}$  exposure ages of K-feldspars from  $^{10}\text{Be}$ -dated moraine boulders yields excellent agreement, confirming the validity of the new SLHL  $^{36}\text{P}_{\text{K-sp}}$  for surface exposure studies, involving  $^{36}\text{Cl}$  in K-feldspars, in the Alps.  
Copyright © 2014 John Wiley & Sons, Ltd.

**KEYWORDS:** European Alps; exposure dating; *in situ* cosmogenic chlorine-36; K-feldspar; production rate calibration

## Introduction

Exposure dating of glacial landforms analysing single ( $^{10}\text{Be}$ ) or multiple ( $^{10}\text{Be}$ ,  $^{26}\text{Al}$ ,  $^{14}\text{C}$ ) *in situ* cosmogenic nuclides in quartz is widely used for reconstructing glacial chronologies (Balco, 2011; Goehring *et al.*, 2011). Although  $^{36}\text{Cl}$  bears the potential to be included in multi-nuclide dating studies owing to its high production in K-feldspars (a mineral often coexisting with quartz in granitic rocks), the precision, accuracy and reliability of  $^{36}\text{Cl}$  exposure dating remains hindered by the uncertainties of the various production pathways of  $^{36}\text{Cl}$ . Thus, the use of  $^{36}\text{Cl}$  in glacial geology has focused primarily on dating moraine boulders without quartz, with particular emphasis on volcanic whole-rock analyses (e.g. Sarikaya *et al.*, 2009). Application of  $^{36}\text{Cl}$  in silicate lithologies poses two major challenges. The first lies in discriminating the numerous production reactions that lead to  $^{36}\text{Cl}$  accumulation in a rock or mineral phase (Schimmelpfennig *et al.*, 2009). There are three types of cosmogenic production pathways for  $^{36}\text{Cl}$ : spallation of K, Ca, Ti and Fe, capture of slow muons by Ca and K, and capture of thermal and epithermal (i.e. low-energy) neutrons by  $^{35}\text{Cl}$ . A non-cosmogenic source is nucleogenic  $^{36}\text{Cl}$  production via low-energy neutron capture and alpha particle interactions resulting from the U–Th decay chain. Estimating the sample-specific low-energy neutron flux responsible for the two latter  $^{36}\text{Cl}$  production reactions is particularly difficult (Phillips *et al.*, 2001) and might intro-

duce substantial uncertainty in calculated  $^{36}\text{Cl}$  ages if the sample's  $^{35}\text{Cl}$  concentration is high (>~ $10^2$  p.p.m.; Schimmelpfennig *et al.*, 2009).

The second difficulty arises from the fact that, to accurately convert measured  $^{36}\text{Cl}$  concentrations into exposure ages, it is important to know the physical parameters underlying the  $^{36}\text{Cl}$  *in situ* production – most importantly the production rate for spallation reactions (number of atoms  $^{36}\text{Cl}$  produced per gram of target element per year). However, published  $^{36}\text{Cl}$  production rates from spallation of K and Ca, when scaled to the conventional reference position at sea level and high latitude (SLHL), reveal discrepancies of up to >50% (Zreda *et al.*, 1991; Stone *et al.*, 1996; Evans *et al.*, 1997; Phillips *et al.*, 2001; Swanson and Caffee, 2001; Licciardi *et al.*, 2008; Schimmelpfennig *et al.*, 2011; Marrero, 2012). Estimates of the  $^{36}\text{Cl}$  production rates from spallation of K (hereafter  $^{36}\text{P}_{\text{K-sp}}$ ) scaled to SLHL range from  $106 \pm 8$  atoms  $^{36}\text{Cl} (\text{gK})^{-1} \text{a}^{-1}$  (Zreda *et al.*, 1991) to  $228 \pm 18$  atoms  $^{36}\text{Cl} (\text{gK})^{-1} \text{a}^{-1}$  (Swanson and Caffee, 2001) (Fig. 1a; Schimmelpfennig *et al.*, 2009, 2011), hampering reliable determination of  $^{36}\text{Cl}$  exposure ages from K-feldspars. While some of the previous  $^{36}\text{P}_{\text{K-sp}}$  calibrations were performed with whole rocks containing various target elements for  $^{36}\text{Cl}$  production and aimed at calibrating several production parameters simultaneously (Zreda *et al.*, 1991; Phillips *et al.*, 2001; Swanson and Caffee, 2001; Fig. 1a), others used K-feldspars with the goal to maximize  $^{36}\text{Cl}$  production from K-spallation (Evans *et al.*, 1997; Schimmelpfennig *et al.*, 2011; Marrero, 2012; Fig. 1a). This 'quasi-single-target' approach has the advantage that it allows minimizing uncertainties resulting from the complex process of deconvoluting the production systematics. Another challenge arises from the rarity of quasi-single-target material in pristine surfaces with robust age control.

\*Correspondence: I. Schimmelpfennig, at <sup>†</sup>Present address below.

E-mail: schimmel@cerege.fr

<sup>†</sup>Present address: CEREGE, Europôle de l'Arbois, BP 80, 13545 Aix-en-Provence, France

<sup>‡</sup>ASTER Team: Maurice Arnold, Georges Aumaître, Didier Bourlès, Karim Keddadouche

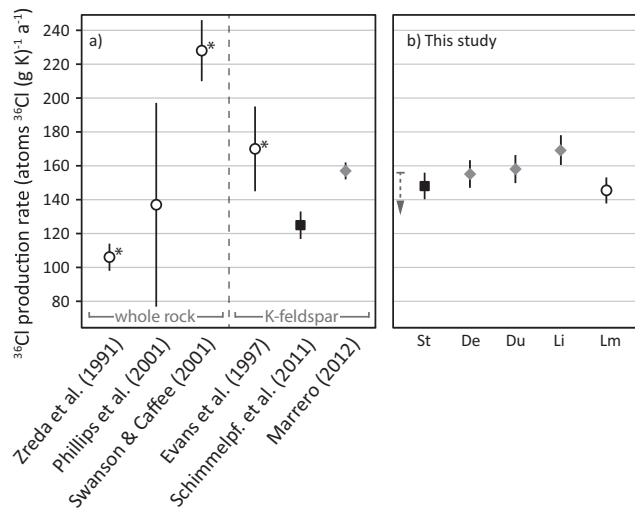


**Figure 1.**  $^{36}\text{Cl}$  production rates from spallation of potassium, referenced to SLHL, derived in previous studies (a) and in this study (b). Open circles refer to the scaling scheme of Lal (1991) (time-dependent implementation: Lm), black squares refer to that by Stone (2000) (St) and grey diamonds represent other scaling schemes (De: Desilets *et al.*, 2006; Du: Dunai, 2001; Li: Lifton *et al.*, 2008). Marrero (2012) used the 'LSD' scaling method of Lifton *et al.* (2014); see note in Supporting information, Appendix S1, Section 2. 'Whole rock' and 'K-feldspar' refers to the calibration material used. The uncertainties in the value by Phillips *et al.* (2001) are given in Marrero (2012), no uncertainties were published in the original paper. \*Values that were not explicitly corrected for muogenic  $^{36}\text{Cl}$  production, which can account for up to  $\sim 5\%$  of total  $^{36}\text{Cl}$  production from K (spallation and muon-capture) depending on altitude. The downward pointing arrow in (b) indicates that the production rates are maximum values.

In this study, we improve the knowledge of  $^{36}\text{P}_{\text{K-sp}}$  based on a quasi-single-target calibration. We use feldspars with K being by far the most abundant  $^{36}\text{Cl}$  target element. The samples are derived from boulders deposited by a prominent landslide near Chironico in the Ticino River valley, South-

Central Swiss Alps (Fig. 2). The landslide event is dated to  $\sim 13.4$  cal ka BP, based on  $^{14}\text{C}$  ages from organic material found at the base of a lacustrine sediment sequence in direct geomorphic relation with the landslide debris (Antognini and Volpers, 2002). This site also forms the basis for an ongoing  $^{10}\text{Be}$  production rate-calibration study, which will be reported in a subsequent paper. We calculate local  $^{36}\text{Cl}$  production rates for each sample (total and K-spallation rates) and use five scaling methods to derive the conventional SLHL values. As a crosscheck of our new  $^{36}\text{P}_{\text{K-sp}}$ , we measure  $^{36}\text{Cl}$  concentrations from K-feldspar-bearing boulder samples of the Tsidjiore Nouve Glacier moraines in the south-western Swiss Alps and compare the resulting  $^{36}\text{Cl}$  exposure ages with  $^{10}\text{Be}$  ages presented by Schimmelpfennig *et al.* (2012).

## Calibration site

The geomorphological setting of the study area is described in detail in Antognini and Volpers (2002) and Claude (2012). The Chironico landslide deposit consists of two granitic gneiss boulder fields located in the centre of the NNW–SSE-trending Leventina valley in the Central Swiss Alps ( $46.4^\circ\text{N}$ ; Fig. 2a). At its northern end, the deposit dammed the Ticino River resulting in the formation of a lake that filled the valley basin with  $\geq 30$  m of lacustrine sediments (Antognini and Volpers, 2002). Antognini and Volpers (2002) collected three wood fragments at almost 40-m depth in a drill core (location in Fig. 2a; schematic log in Fig. 2b), about 6 m (samples MCSN-1 and -2) and 6.5 m (sample MCSN-3) above the bottom of the lake sediment sequence. They obtained radiocarbon ages of  $11\,340 \pm 80$   $^{14}\text{C}$  a BP (MCSN-1),  $11\,690 \pm 85$   $^{14}\text{C}$  a BP (MCSN-2), and  $11\,500 \pm 80$   $^{14}\text{C}$  a BP (MCSN-3) (Fig. 2b), from which the respective calibrated ages and  $1\sigma$  errors, using OxCal 4.2 and the IntCal13 calibration dataset (Bronk Ramsey, 2009, 2013; Reimer *et al.*, 2013), are  $13\,195 \pm 74$ ,  $13\,526 \pm 93$  and  $13\,340 \pm 80$  cal a BP. Sample MCSN-1 is slightly younger than the others, although it is

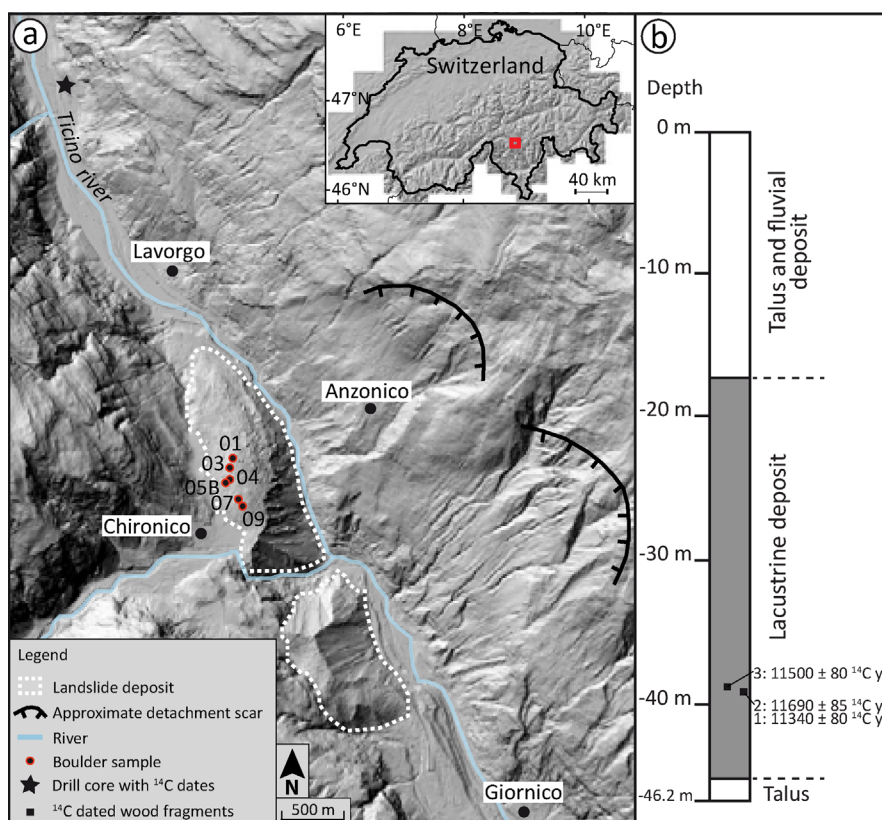


**Figure 2.** Chironico calibration site. (a) Geomorphic map of the area on an ALTI3D model by Swisstopo<sup>®</sup>. Inset highlights location of study area in red. Calibration sample locations are shown on northern landslide deposit with short form of sample labels CHI-11-xx. (b) Schematic log of drill core with depth of  $^{14}\text{C}$ -dated wood fragments and uncalibrated  $^{14}\text{C}$  ages, simplified after Antognini and Volpers (2002). Numbers 1, 2 and 3 are short form of sample labels MCSN-x. This figure is available in colour online at [wileyonlinelibrary.com](http://wileyonlinelibrary.com).

stratigraphically lower than MCSN-3. We therefore calculated the mean and standard deviation of these three calibrated dates,  $13\,350 \pm 170$  cal a BP. Instead of the conventional radiocarbon reference year CE 1950, we report the calibrated age relative to CE 2011, the year of boulder sampling, resulting in an age of  $13\,410 \pm 170$  cal a BP.

Because the time lag between the landslide event and the deposition of the dated wood fragments is unknown, the date strictly provides a minimum age for the beginning of exposure of the debris boulders to cosmic radiation. Production rates derived from the landslide boulders must therefore be considered as upper bounds of the actual rates. However, we assume the time lag to be small based on the observation that lakes contemporarily dammed by landslides in mountain valleys are rapidly filled with sediment ( $\sim 10^1$ – $10^2$  years; e.g. Adams, 1981). In addition, Antognini and Volpers (2002) tentatively estimated that the lake persisted for only a few hundred years (between 120 and 730 years), based on the calculated volume of sediment stored in the dammed lake and on post-Last Glacial Maximum and modern lake sedimentation rates in the study site catchment. Assuming immediate onset of lake sedimentation after the landslide, the upper-bound duration of 730 years for the lake's life time and a constant sedimentation rate, the dated wood fragments would have been deposited  $\sim 160$  years after the landslide. This duration is similar to the standard deviation of the calibrated <sup>14</sup>C mean age. It is therefore likely that this mean age is a close minimum age for the landslide event and thus for the beginning of boulder exposure.

### Methods

At the Chironico landslide deposit, surface samples with thicknesses of 1–4 cm were collected from the top part of nine 2–4-m-tall, well-embedded orthogneiss boulders following methods in Putnam *et al.* (2010) (supporting Fig. S1). Five of the surface samples had enough K-feldspar for <sup>36</sup>Cl extractions. The boulders are located at elevations between 815 and 827 m. Signs of significant erosion were not evident on the sampled surfaces. In addition to the boulder surfaces, sample CHI-10-05B was taken from the bottom of a 2.5–3-m-high and  $\sim 7$ -m-wide boulder (supporting Fig. S1) to test whether nuclide concentrations from exposure of the rock material in the cliff wall before the landslide (pre-exposure) might bias the calibration. We note that the surface sample from boulder CHI-10-05 did not have any K-feldspar preventing us from directly comparing <sup>36</sup>Cl concentrations in the bottom and surface samples of the same boulder.

<sup>36</sup>Cl extractions follow the procedure described by Schimmelpfennig *et al.* (2011) (details in supporting Appendix S1, section 1). Sample details and chemical data are shown in Table 1.

All <sup>36</sup>Cl production-related calculations are done using the <sup>36</sup>Cl Excel<sup>®</sup> calculation spreadsheet published by Schimmelpfennig *et al.* (2009), which allows deriving the SLHL <sup>36</sup>Cl production rate from spallation of K (SLHL <sup>36</sup>P<sub>K-sp</sub>) (Table 2) by minimizing, through adjustment of the SLHL <sup>36</sup>P<sub>K-sp</sub> value, the misfit between the measured <sup>36</sup>Cl concentration and the total calculated <sup>36</sup>Cl concentration (sum of contributions from all production reactions, Table 3).

We also derive local <sup>36</sup>Cl production rates for each sample, first the local *total* <sup>36</sup>Cl production rate (<sup>36</sup>P<sub>total</sub>) and then the local *K-spallation* <sup>36</sup>Cl production rate (<sup>36</sup>P<sub>K-sp</sub>) (Table 2).

The local <sup>36</sup>P<sub>total</sub> includes the <sup>36</sup>Cl production from all target elements present in the minerals and is therefore

**Table 1A.** Sample-specific details and target element concentrations of calibration and moraine samples.

Sample	Latitude (°N)	Longitude (°E)	Altitude (m)	Thickness (cm)	Shielding factor	Sample weight (g)	K (%)	Ca (%)	Ti (%)	Fe (%)
Chironico calibration samples										
CHI-11-01	46.42841	8.84651	824.0	2.5	0.978	12.75	9.45 ± 0.19	0.440 ± 0.022	0.013 ± 0.001	0.040 ± 0.006
CHI-11-03	46.42773	8.84660	827.4	2.6	0.981	13.42	11.46 ± 0.23	0.094 ± 0.009	<d.l.	0.051 ± 0.008
CHI-11-04	46.42694	8.84624	817.3	2.0	0.979	14.12	10.71 ± 0.21	0.110 ± 0.011	0.017 ± 0.002	0.064 ± 0.010
CHI-11-07	46.42556	8.84708	824.4	3.1	0.978	15.78	9.41 ± 0.32	0.449 ± 0.055	0.007 ± 0.012	0.052 ± 0.016
CHI-11-09	46.42506	8.84753	819.7	1.9	0.982	28.18	8.85 ± 0.31	0.311 ± 0.077	0.003 ± 0.006	0.061 ± 0.003
CHI-11-05B	46.42674	8.84583	814.8	1.7	0.979	6.70	8.82 ± 0.18	0.367 ± 0.018	0.015 ± 0.006	0.045 ± 0.007
Moraine samples Tsidjore Nouve Glacier										
ARO-56	46.01798	7.46267	2419	3.3	0.974	17.08	10.72 ± 0.21	0.034 ± 0.003	<d.l.	<d.l.
ARO-16	46.01777	7.46387	2399	1.6	0.954	13.13	6.68 ± 0.13	0.059 ± 0.006	<d.l.	0.022 ± 0.003
ARO-12	46.01678	7.46504	2416	3.2	0.981	12.95	10.62 ± 0.21	0.038 ± 0.004	<d.l.	0.071 ± 0.004

Concentrations of target elements K, Ca, Ti and Fe were determined by ICP-OES (for details see supporting Appendix S1, Section 1). <d.l., below detection limit.

**Table 1B.**  $^{36}\text{Cl}$  and Cl data of calibration and moraine samples.

	Cl mass in spike (mg)	$^{35}\text{Cl}/^{37}\text{Cl}$	$^{36}\text{Cl}/^{35}\text{Cl}$ ( $10^{-13}$ )	[Cl] in sample (p.p.m.)	$^{36}\text{Cl}$ ( $10^3$ atoms $\text{g}^{-1}$ )
Chironico calibration samples					
CHI-11-01	1.522	$86.85 \pm 0.69$	$1.891 \pm 0.063$	$4.6 \pm 0.1$	$390 \pm 13$
CHI-11-03	1.512	$30.14 \pm 0.29$	$2.194 \pm 0.071$	$16.1 \pm 0.2$	$462 \pm 15$
CHI-11-04	1.512	$41.31 \pm 0.60$	$2.164 \pm 0.067$	$10.5 \pm 0.2$	$420 \pm 14$
CHI-11-07	1.513	$77.3 \pm 2.5$	$2.404 \pm 0.077$	$4.4 \pm 0.2$	$401 \pm 13$
CHI-11-09	1.510	$65.0 \pm 2.2$	$4.01 \pm 0.12$	$3.1 \pm 0.1$	$381 \pm 12$
CHI-11-05B	1.517	$124.7 \pm 5.1$	$0.121 \pm 0.012$	$5.2 \pm 0.3$	$26.7 \pm 5.9$
Moraine samples Tsidjiore Nouve Glacier					
ARO-56	1.818	$26.77 \pm 0.57$	$5.83 \pm 0.31$	$18.0 \pm 0.5$	$1196 \pm 66$
ARO-16	1.715	$20.75 \pm 0.28$	$3.06 \pm 0.25$	$29.9 \pm 0.5$	$794 \pm 66$
ARO-12	1.798	$23.50 \pm 0.20$	$1.527 \pm 0.059$	$27.4 \pm 0.3$	$407 \pm 16$
Blanks (processed with)					
				Total atoms $^{36}\text{Cl}$ ( $10^{16}$ )	Total atoms $^{36}\text{Cl}$ ( $10^{15}$ )
Blank-IS-05Jun13 (CHI-11-01, -03, -04, -05 B)	1.517	$373.2 \pm 6.6$	$0.0548 \pm 0.0083$	$16.36 \pm 0.51$	$1.44 \pm 0.22$
Bl-2012Aug16-1 (CHI-11-07, -09)	1.516	$469 \pm 15$	$0.0563 \pm 0.0092$	$12.23 \pm 0.71$	$1.47 \pm 0.24$
Bl-2012Aug16-2 (CHI-11-07, -09)	1.520	$389 \pm 12$	$0.069 \pm 0.011$	$17.07 \pm 0.82$	$1.80 \pm 0.28$
Bl-IS-9Dec13 (ARO-56, -16, -12)	1.810	$601 \pm 38$	$0.0497 \pm 0.0078$	$5.5 \pm 1.3$	$1.55 \pm 0.24$

$^{36}\text{Cl}$  and Cl data are from isotope dilution AMS measurements at ASTER-CEREGE, normalized to a  $^{36}\text{Cl}$  standard prepared by K. Nishiizumi (Sharma *et al.*, 1990), assuming a natural  $^{35}\text{Cl}/^{37}\text{Cl}$  ratio of 3.127. Spike enriched in  $^{35}\text{Cl}$  ( $\sim 99.9\%$ ).

composition (i.e. sample) dependent. It is estimated as follows:

$$^{36}P_{\text{total}} = \frac{(N_{\text{meas}} - N_{\text{nucl}}) \frac{1}{S_T} \frac{1}{e^{-d/\Lambda}}}{(1 - e^{-t_{\text{exp}} \lambda_{36}}) / \lambda_{36}}$$

where  $N_{\text{meas}}$  is the measured  $^{36}\text{Cl}$  concentration,  $N_{\text{nucl}}$  the nucleogenic  $^{36}\text{Cl}$  contribution,  $S_T$  the topographic shielding factor,  $1/e^{-d/\Lambda}$  the sample thickness correction factor,  $t_{\text{exp}}$  the independently determined exposure time and  $\lambda_{36}$  the decay constant of  $^{36}\text{Cl}$  ( $2.303 \times 10^{-6} \text{ a}^{-1}$ ).

The local  $^{36}P_{\text{K-sp}}$  excludes the  $^{36}\text{Cl}$  contributions from all production reactions other than K-spallation and is normalized to the concentration of K in each sample. It is inferred as follows:

$$^{36}P_{\text{K-sp}} = \frac{(N_{\text{meas}} - N_{\text{non-K-sp}}) \frac{1}{S_T} \frac{1}{e^{-d/\Lambda}}}{N_K (1 - e^{-t_{\text{exp}} \lambda_{36}}) / \lambda_{36}}$$

where  $N_{\text{non-K-sp}}$  is the sum of the  $^{36}\text{Cl}$  concentrations estimated for all production reactions other than K-spallation at the calibration site [these concentrations are based on sample composition, published SLHL production parameters, the scaling schemes cited below and the exposure time, and represent minor contributions mostly from low-energy neutron capture by  $^{35}\text{Cl}$  ( $\leq 3\%$ ), muon capture by K ( $\leq 2.3\%$ ) and nucleogenic  $^{36}\text{Cl}$  production ( $\leq 3.1\%$ , Table 3), and  $N_K$  the concentration of K [ $\text{g} (\text{g rock})^{-1}$ ].

The SLHL  $^{36}P_{\text{K-sp}}$  of each sample corresponds to the local  $^{36}P_{\text{K-sp}}$  divided by the site-specific spallation scaling factor, which we derived from the five most commonly used scaling schemes, hereafter referred to as St (Stone, 2000), De (Desilets *et al.*, 2006), Du (Dunai, 2001), Li (Lifton *et al.*, 2008) and Lm (time-dependent version of Lal, 1991), following the convention set by Balco *et al.* (2008) (details in supporting Appendix S1, Section 2 and supporting Table S2). The uncertainties ( $1\sigma$ ) taken into account in all production parameters and sample-specific variables are detailed in supporting Appendix S1, Section 3 and fully propagated into the  $^{36}\text{Cl}$  production rates.

**Table 2.**  $^{36}\text{Cl}$  production rates from Chironico calibration samples.

Sample	Local $^{36}P_{\text{total}}$ [atoms $^{36}\text{Cl}$ $\text{g}^{-1} \text{ a}^{-1}$ ]	Local $^{36}P_{\text{K-sp}}$ [atoms $^{36}\text{Cl}$ $(\text{g K})^{-1} \text{ a}^{-1}$ ]	SLHL $^{36}P_{\text{K-sp}}$ St [atoms $^{36}\text{Cl}$ $(\text{g K})^{-1} \text{ a}^{-1}$ ]	SLHL $^{36}P_{\text{K-sp}}$ De [atoms $^{36}\text{Cl}$ $(\text{g K})^{-1} \text{ a}^{-1}$ ]	SLHL $^{36}P_{\text{K-sp}}$ Du [atoms $^{36}\text{Cl}$ $(\text{g K})^{-1} \text{ a}^{-1}$ ]	SLHL $^{36}P_{\text{K-sp}}$ Li [atoms $^{36}\text{Cl}$ $(\text{g K})^{-1} \text{ a}^{-1}$ ]	SLHL $^{36}P_{\text{K-sp}}$ Lm [atoms $^{36}\text{Cl}$ $(\text{g K})^{-1} \text{ a}^{-1}$ ]
CHI-11-01	$30.4 \pm 1.0$	$308 \pm 13$	$148.9 \pm 6.4$	$156.1 \pm 6.7$	$159.0 \pm 6.8$	$170.3 \pm 7.3$	$146.3 \pm 6.3$
CHI-11-03	$35.3 \pm 1.2$	$291 \pm 12$	$140.6 \pm 6.0$	$147.5 \pm 6.3$	$150.3 \pm 6.4$	$161.1 \pm 6.9$	$138.1 \pm 5.9$
CHI-11-04	$32.2 \pm 1.0$	$287 \pm 12$	$139.6 \pm 5.8$	$146.4 \pm 6.0$	$149.2 \pm 6.1$	$159.9 \pm 6.6$	$137.2 \pm 5.7$
CHI-11-07	$31.5 \pm 0.8$	$320 \pm 11$	$155.0 \pm 5.5$	$162.5 \pm 5.8$	$165.5 \pm 5.9$	$177.3 \pm 6.3$	$152.3 \pm 5.4$
CHI-11-09	$29.6 \pm 0.7$	$322 \pm 11$	$156.4 \pm 5.4$	$164.0 \pm 5.7$	$167.0 \pm 5.8$	$178.8 \pm 6.2$	$153.8 \pm 5.3$
Summary statistics							
Arithmetic mean		$306 \pm 16$	$148.1 \pm 7.8$	$155.3 \pm 8.2$	$158.2 \pm 8.3$	$169.5 \pm 8.8$	$145.5 \pm 7.7$
Weighted mean		$307 \pm 5$	$148.6 \pm 2.6$	$155.7 \pm 2.7$	$158.6 \pm 2.8$	$170.0 \pm 3.0$	$146.0 \pm 2.5$
Reduced $\chi^2$		2.0	1.9	1.9	1.9	1.8	1.9

The local total  $^{36}\text{Cl}$  production rates (local  $^{36}P_{\text{total}}$ ) are composition-dependent and therefore not averaged. The  $^{36}\text{Cl}$  production rates from spallation of K (local  $^{36}P_{\text{K-sp}}$ ) were derived by subtracting the site- and sample-specific  $^{36}\text{Cl}$  concentrations calculated for all  $^{36}\text{Cl}$  production reactions other than spallation of K from the measured  $^{36}\text{Cl}$  concentrations. Note that the  $^{36}\text{Cl}$  contributions from these other reactions were scaled to the sample site using the Lm method. Using other scaling methods would change the local  $^{36}P_{\text{K-sp}}$  by  $< 1\%$ . The local  $^{36}P_{\text{K-sp}}$  values of all samples are averaged over a small range of altitudes (817–827 m), corresponding to a relative production rate difference of  $< 1\%$  (scaling factors in supporting Table S2). The  $^{36}\text{Cl}$  production rates from spallation of K referenced to sea level and high latitude (SLHL  $^{36}P_{\text{K-sp}}$ ) are derived using the scaling methods of Stone (2000) (St), Desilets *et al.* (2006) (De), Dunai (2001) (Du), Lifton *et al.* (2008) (Li) and Lal (1991), accounting for temporal geomagnetic variations (Lm). See text for further details.

**Table 3.** Relative <sup>36</sup>Cl contributions from the various production reactions to total <sup>36</sup>Cl concentrations in the calibration and moraine samples.

Production pathway	<sup>36</sup> Cl contributions in Chironico calibration K-feldspars	<sup>36</sup> Cl contributions in K-feldspars from moraine samples	Default values for production rates and parameters at SLHL	Reference
Spallation of K	92–96%	88–94%	145.5 ± 7.7 atoms <sup>36</sup> Cl (g K) <sup>-1</sup> a <sup>-1</sup>	This study
Spallation of Ca	0.2–1.3%	0.1–0.2%	42.2 ± 4.8 atoms <sup>36</sup> Cl (g Ca) <sup>-1</sup> a <sup>-1</sup>	Schimmelpfennig <i>et al.</i> , 2011
Spallation of Ti	≤0.01%	0%	13 ± 3 atoms <sup>36</sup> Cl (g Ti) <sup>-1</sup> a <sup>-1</sup>	Fink <i>et al.</i> , 2000
Spallation of Fe	0.01%	≤0.01%	1.9 ± 0.2 atoms <sup>36</sup> Cl (g Fe) <sup>-1</sup> a <sup>-1</sup>	Stone <i>et al.</i> , 2005
Low-energy neutron capture by <sup>35</sup> Cl	0.6–2.8%	3.6–8.2%	626 neutrons (g air) <sup>-1</sup> a <sup>-1</sup>	Phillips <i>et al.</i> , 2001
Slow muon capture by K and Ca	2.2–2.3%	1.3%	190 μg <sup>-1</sup> a <sup>-1</sup>	Heisinger <i>et al.</i> , 2002
Nucleogenic production	0.8–3.1%	1.1–4.5%		

The relative contributions are the proportions of the calculated <sup>36</sup>Cl concentrations from each production reaction in the total measured <sup>36</sup>Cl concentration of each sample. The contributions are derived using the <sup>36</sup>Cl Excel<sup>®</sup> calculation spreadsheet published by Schimmelpfennig *et al.* (2009). The spreadsheet allows us to calculate the <sup>36</sup>Cl concentrations from each production reaction based on the respective target element concentration, the production parameter scaled to the site of interest (SLHL production parameters can be changed by the user, and scaling factors must be provided by the user), sample-related correction factors (shielding, thickness, rock density) and the independently determined exposure time. Here we use the SLHL production parameters given in the table and the scaling scheme by Lal (1991). Note that the relative <sup>36</sup>Cl contributions change insignificantly when using other scaling schemes. Details and equations of all calculations are given in Schimmelpfennig *et al.* (2009).

## Results

The concentrations of K of ~9–12% are substantially higher than those of any other <sup>36</sup>Cl target element in our samples (Table 1) and therefore allow the maximization of <sup>36</sup>Cl contribution from K-spallation to ≥92%, largely outweighing minor contributions from the other production reactions (Table 3).

The <sup>36</sup>Cl concentrations in the five calibration samples range from 381 ± 12 × 10<sup>3</sup> to 462 ± 15 × 10<sup>3</sup> atoms g<sup>-1</sup>. These <sup>36</sup>Cl concentrations positively correlate with the concentrations of K (Table 1), as is expected for surfaces at similar altitude and of the same exposure history. This indicates that none of the boulders bears significant <sup>36</sup>Cl concentrations inherited from pre-exposure on the cliff, because it is unlikely that all five boulders were buried at the same shallow depth in the wall, otherwise more scatter would be expected. In addition, assuming that the boulder from which bottom sample CHI-10-05B was taken came from a similarly deep position in the wall as the other boulders, we use the <sup>36</sup>Cl concentration measured in this bottom sample to check the likeliness that this concentration has partly accumulated during pre-exposure on the cliff. This concentration is ~26.7 ± 5.9 × 10<sup>3</sup> atoms <sup>36</sup>Cl g<sup>-1</sup> (Table 1). Estimating the concentration at 2.5-m depth of this boulder, that would be expected to have accumulated since the emplacement of the landslide, yields ~16 ± 5 × 10<sup>3</sup> atoms <sup>36</sup>Cl g<sup>-1</sup>. The difference between measured and estimated concentrations is thus ~11 ± 8 × 10<sup>3</sup> atoms <sup>36</sup>Cl g<sup>-1</sup>, which accounts for ~2% of the mean <sup>36</sup>Cl concentration in the surface samples of the other boulders. This small proportion implies that pre-exposure is probably negligible. We further note that the <sup>36</sup>Cl contribution from muon capture in our K-rich minerals is low (~2%; Table 3) and therefore does not constitute a significant potential source for <sup>36</sup>Cl concentrations inherited from pre-exposure at depth in the cliff, which has to be considered in Ca-rich lithologies (Sadier *et al.*, 2012).

The local <sup>36</sup>P<sub>total</sub> at the Chironico site, including all cosmogenic production reactions in the minerals, range from 29.6 ± 1.3 to 35.3 ± 1.4 atoms <sup>36</sup>Cl (g sample)<sup>-1</sup> a<sup>-1</sup> (Table 2) for the compositions of the five K-feldspar samples (Table 1). The local <sup>36</sup>P<sub>K-sp</sub> values are between 287 ± 12 and 320 ± 11 atoms <sup>36</sup>Cl (g K)<sup>-1</sup> a<sup>-1</sup> with an arithmetic mean and standard deviation of 306 ± 16 atoms <sup>36</sup>Cl (g K)<sup>-1</sup> a<sup>-1</sup> (Table 2). Note

the different units of the local <sup>36</sup>P<sub>total</sub> and the local <sup>36</sup>P<sub>K-sp</sub>, and that the local <sup>36</sup>P<sub>K-sp</sub> is an order of magnitude higher than the local <sup>36</sup>P<sub>total</sub>, because the concentration of K is about 10% in our samples (Table 1).

Finally, scaled to SLHL, the arithmetic mean <sup>36</sup>P<sub>K-sp</sub> ranges between 145.5 ± 7.7 atoms <sup>36</sup>Cl (g K)<sup>-1</sup> a<sup>-1</sup> (Lm scaling) and 169.5 ± 8.8 atoms <sup>36</sup>Cl (g K)<sup>-1</sup> a<sup>-1</sup> (Li scaling) (Table 2, Fig. 1b and supporting Fig. S2).

## Comparison with previous K-spallation <sup>36</sup>Cl production rate calibrations

Here, we focus on the SLHL <sup>36</sup>P<sub>K-sp</sub> results according to the St and Lm scaling schemes (yielding similar values of 148.1 ± 7.8 and 145.5 ± 7.7 atoms <sup>36</sup>Cl (g K)<sup>-1</sup> a<sup>-1</sup>, respectively), because previous SLHL <sup>36</sup>P<sub>K-sp</sub> values were scaled with the methods of Lal (1991) or Stone (2000), except the value by Marrero (2012), who applied the ‘LSD’ method of Lifton *et al.* (2014). We note that the scaling predictions from the LSD model are similar to those from the Lm model at the Chironico site as well as at the two <sup>36</sup>P<sub>K-sp</sub> calibration sites in Marrero (2012) (Scotland, 300 m, 57°N and Huanacané, Peru, 4900 m, 14°S) according to fig. 1 in Lifton *et al.* (2014) (also see note in supporting Appendix S1, Section 2).

Figure 1 compares the SLHL <sup>36</sup>P<sub>K-sp</sub> previously derived from both whole rocks and K-feldspars (Fig. 1a) with the new results from Chironico (Fig. 1b). While the values from whole rocks show considerable scatter and are either significantly lower or significantly higher than our results (and one is poorly constrained with ~44% uncertainty), there is excellent agreement between the SLHL <sup>36</sup>P<sub>K-sp</sub> from Chironico and those obtained by Marrero (2012) (157 ± 6 atoms <sup>36</sup>Cl (g K)<sup>-1</sup> a<sup>-1</sup>) and Evans *et al.* (1997) (170 ± 25 atoms <sup>36</sup>Cl (g K)<sup>-1</sup> a<sup>-1</sup>), all derived from K-feldspars. This result attests to the validity of the quasi-single-target approach using K-feldspars for the calibration of SLHL <sup>36</sup>P<sub>K-sp</sub>. Another SLHL <sup>36</sup>P<sub>K-sp</sub> calibration result of 124.9 ± 8.1 atoms <sup>36</sup>Cl (g K)<sup>-1</sup> a<sup>-1</sup>, principally based on K-feldspars from a lava flow in Argentina (~2400 m, 38°S) with similarly high <sup>36</sup>Cl contribution from K-spallation (>90%) (Schimmelpfennig *et al.*, 2011), is ~16% lower than the results presented here. The most likely explanation for this divergence is that the independent age of the flow, determined by K–Ar dating to

15.2 ± 0.9 ka, is overestimated. Further possible reasons include unrecognized erosion of the lava flow, which would reduce the surface  $^{36}\text{Cl}$  concentrations and result in an underestimated production rate, or that the common scaling methods poorly describe the variability of  $^{36}\text{P}_{\text{K-sp}}$  at this Southern Hemisphere mid-altitude site.

## Crosscheck with $^{10}\text{Be}$ moraine boulder ages

We measured  $^{36}\text{Cl}$  in three K-feldspar samples remaining from a  $^{10}\text{Be}$  moraine dating study at the Tsidjiore Nouve Glacier in the Swiss Alps (2400 m, 46.0°N; Schimmelpfennig *et al.*, 2012) (sample details in Table 1). The compositions are similar to those of the Chironico K-feldspars (Table 1), and  $^{36}\text{Cl}$  production from K-spallation accounts for ≥88% of total  $^{36}\text{Cl}$  production (Table 3). The  $^{10}\text{Be}$  ages were derived using the  $^{10}\text{Be}$  production rate of Balco *et al.* (2009) (north-eastern North America data set) and the Lm scaling, yielding 11.14 ± 0.59, 10.96 ± 0.58 and 3.78 ± 0.2 ka. Using the Chironico SLHL  $^{36}\text{P}_{\text{K-sp}}$  (Lm) in the  $^{36}\text{Cl}$  exposure age calculations of the moraine K-feldspars results in 11.3 ± 1.3, 11.1 ± 1.1 and 3.58 ± 0.32 ka, respectively, which is in excellent agreement with the  $^{10}\text{Be}$  ages (Fig. 3). This implies that the Chironico SLHL  $^{36}\text{P}_{\text{K-sp}}$  and Balco *et al.*'s (2009)  $^{10}\text{Be}$  production rate are compatible and likely to be valid on a regional basis in the Alps.

## Conclusions

Based on the  $^{14}\text{C}$ -dated Chironico landslide calibration site in the Swiss Alps, we present a new  $^{36}\text{Cl}$  production rate from K-spallation inferred from quasi-single-target K-feldspars ( $^{36}\text{Cl}$  from K-spallation maximized to >92%). The local  $^{36}\text{P}_{\text{K-sp}}$  mean value is 306 ± 16 atoms  $^{36}\text{Cl}$  (g K) $^{-1}$  a $^{-1}$  and the SLHL  $^{36}\text{P}_{\text{K-sp}}$  mean value is 145.5 ± 7.7 atoms  $^{36}\text{Cl}$  (g K) $^{-1}$  a $^{-1}$  (Lm scaling). The good agreement with SLHL  $^{36}\text{P}_{\text{K-sp}}$  previously calibrated with K-feldspars supports both the robustness of the quasi-single-target strategy for  $^{36}\text{Cl}$  production rate calibrations, and the likelihood that our new SLHL  $^{36}\text{P}_{\text{K-sp}}$ , which is a maximum production rate, is close to the true value.

We also present  $^{36}\text{Cl}$  moraine ages almost entirely based on  $^{36}\text{Cl}$  production from K-spallation. The results agree strikingly well with  $^{10}\text{Be}$  moraine ages published previously. These findings highlight that  $^{36}\text{Cl}$  dating is now possible with improved precision and accuracy for studies of glacial landforms when using K-feldspars. This is of particular interest for lithologies with rare quartz but abundant K-feldspar, such as trachytes, and for multi-nuclide applications, in which, for example,  $^{36}\text{Cl}$  analyses in K-feldspars can be combined with  $^{10}\text{Be}$  measurements in quartz from the same samples.

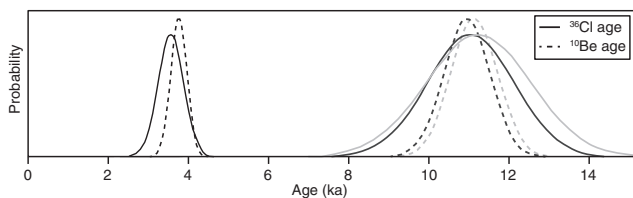


**Figure 3.** Probability plots of  $^{36}\text{Cl}$  ages from K-feldspars (solid lines) and  $^{10}\text{Be}$  ages from quartz (dashed lines) of three boulders on the moraines of the Tsidjiore Nouve Glacier (Schimmelpfennig *et al.*, 2012). Curves plotted in the same shade of grey correspond to the same boulder. All ages are scaled according to the Lm model.  $^{36}\text{Cl}$  ages are calculated using the production rate determined in this study.  $^{10}\text{Be}$  ages are calculated with the production rate of Balco *et al.* (2009). Errors are 1 $\sigma$  and include analytical and production rate uncertainties.

## Supporting Information

Additional supporting information can be found in the online version of this article:

**Appendix S1.** Sample preparation, measurements and calibration approach (Section 1). Determination of scaling factors (Section 2) and Uncertainties (Section 3).

**Table S1.** Bulk rock sample compositions.

**Table S2.** Scaling factors.

**Figure S1.** Photographs of sampled boulders.

**Figure S2.** Summed probability plot of the individual  $^{36}\text{Cl}$  production rates.

**Acknowledgements.** We thank J. Hanley, R. Schwartz and K. Needleman for help with sample preparation. We acknowledge support by the International Balzan Foundation, the German Academic Exchange Service (DAAD), the College de France, the Lamont Climate Center and the Comer Science and Education Foundation. The ASTER French AMS national facility (CEREGE, Aix en Provence) is supported by the INSU/CNRS, the French Ministry of Research and Higher Education, IRD and CEA. We thank the staff at SARM-CRPG for the compositional analysis. Reviewers Jason Briner and David Fink made constructive comments, which significantly improved the manuscript. This is Lamont-Doherty Earth Observatory publication 7793.

**Abbreviation.** SLHL, sea-level/high-latitude.

## References

- Adams J., 1981. Earthquake-dammed lakes in New Zealand. *Geology* **9**: 215–219.
- Antognini M, Volpers R., 2002. A Late Pleistocene age for the Chironico rockslide (Central Alps, Ticino, Switzerland). *Bulletin of Applied Geology* **7**: 113–125.
- Balco G, Stone JO, Lifton NA, *et al.* 2008. A complete and easily accessible means of calculating surface exposure ages or erosion rates from  $^{10}\text{Be}$  and  $^{26}\text{Al}$  measurements. *Quaternary Geochronology* **3**: 174–195.
- Balco G, Briner J, Finkel RC, *et al.* 2009. Regional beryllium-10 production rate calibration for late-glacial northeastern North America. *Quaternary Geochronology* **4**: 93–107.
- Balco G., 2011. Contributions and unrealized potential contributions of cosmogenic-nuclide exposure dating to glacier chronology, 1990–2010. *Quaternary Science Reviews* **30**: 3–27.
- Bronk Ramsey C., 2009. Bayesian analysis of radiocarbon dates. *Radiocarbon* **51**: 337–360.
- Bronk Ramsey C., 2013. OxCal Program 4.2.3, <https://c14.arch.ox.ac.uk/oxcal/OxCal.html>.
- Claude A., 2012. *Geomorphology, age and landscape evolution at the Chironico landslide, Leventina Valley, southern Swiss Alps*. MSc Thesis, ETH Zurich.
- Desilets D, Zreda M, Prabu T., 2006. Extended scaling factors for *in situ* cosmogenic nuclides: new measurements at low latitude. *Earth and Planetary Sciences Letters* **246**: 265–276.
- Dunai T., 2001. Influence of secular variation of the magnetic field on production rates of *in situ* produced cosmogenic nuclides. *Earth and Planetary Sciences Letters* **193**: 197–212.
- Evans JM, Stone JO, Fifield LK, *et al.* 1997. Cosmogenic  $^{36}\text{Cl}$  production in K-feldspar. *Nuclear Instruments and Methods in Physics Research Section B* **123**: 334–340.
- Fink D, Vogt S, Hotchkis M., 2000. Cross-sections for  $^{36}\text{Cl}$  from Ti at  $E_p = 35\text{--}150$  MeV: applications to *in-situ* exposure dating. *Nuclear Instruments and Methods in Physics Research Section B* **172**: 861–866.
- Goehring BM, Schaefer JM, Schluechter C, *et al.* 2011. Rhône Glacier was smaller than today for most of the Holocene. *Geology* **39**: 679–682.
- Heisinger B, Lal D, Jull AJT, *et al.* 2002. Production of selected cosmogenic radionuclides by muons: 2. Capture of negative muons. *Earth and Planetary Sciences Letters* **200**: 357–369.

- Lal D., 1991. Cosmic-ray labeling of erosion surfaces: *in situ* nuclide production rates and erosion models. *Earth and Planetary Sciences Letters* **104**: 424–439.
- Licciardi J, Denoncourt C, Finkel R., 2008. Cosmogenic  $^{36}\text{Cl}$  production rates from Ca spallation in Iceland. *Earth and Planetary Sciences Letters* **267**: 365–377.
- Lifton N, Smart D, Shea M., 2008. Scaling time-integrated *in situ* cosmogenic nuclide production rates using a continuous geomagnetic model. *Earth and Planetary Sciences Letters* **268**: 190–201.
- Lifton N, Sato T, Dunai T., 2014. Scaling *in situ* cosmogenic nuclide production rates using analytical approximations to atmospheric cosmic-ray fluxes. *Earth and Planetary Sciences Letters* **386**: 149–160.
- Marrero S., 2012. *Calibration of cosmogenic chlorine-36*. PhD Thesis, New Mexico Institute of Mining and Technology, Socorro, NM, USA.
- Phillips FM, Stone WD, Fabryka-Martin JT., 2001. An improved approach to calculating low-energy cosmic-ray neutron fluxes near the land/atmosphere interface. *Chemical Geology* **175**: 689–701.
- Putnam AE, Schaefer JM, Barrell DJA, et al. 2010. In situ cosmogenic  $^{10}\text{Be}$  production-rate calibration from the Southern Alps, New Zealand. *Quaternary Geochronology* **5**: 392–409.
- Reimer PJ, Bard E, Bayliss A, et al. 2013. IntCal13 and Marine13 radiocarbon age calibration curves 0–50,000 years cal BP. *Radiocarbon* **55**: 1869–1887.
- Sadier B, Delannoy J.-J, Benedetti L et al. 2012. Further constraints on the Chauvet cave artwork elaboration. *Proceedings of the National Academy of Sciences of the United States of America* **109**: 8002–8006.
- Sarikaya MA, Zreda M, Çiner A., 2009. Glaciations and paleoclimate of Mount Erciyes, central Turkey, since the Last Glacial Maximum, inferred from  $^{36}\text{Cl}$  cosmogenic dating and glacier modeling. *Quaternary Science Reviews* **28**: 2326–2341.
- Schimmelpfennig I, Benedetti L, Finkel R, et al. 2009. Sources of *in situ*  $^{36}\text{Cl}$  in basaltic rocks. Implications for calibration of production rates. *Quaternary Geochronology* **4**: 441–461.
- Schimmelpfennig I, Benedetti L, Garreta V, et al. 2011. Calibration of cosmogenic  $^{36}\text{Cl}$  production rates from Ca and K spallation in lava flows from Mt. Etna (38°N, Italy) and Payun Matru (36°S, Argentina). *Geochimica et Cosmochimica Acta* **75**: 2611–2632.
- Schimmelpfennig I, Schaefer JM, Akçar N, et al. 2012. Holocene glacier culminations in the Western Alps and their hemispheric relevance. *Journal of Geology* **40**: 891–894.
- Sharma P, Kubik PW, Fehn U, et al. 1990. Development of  $^{36}\text{Cl}$  standards for AMS. *Nuclear Instruments and Methods in Physics Research Section B* **52**: 410–415.
- Stone JO., 2000. Air pressure and cosmogenic isotope production. *Journal of Geophysical Research* **105**: 23753–23759.
- Stone JO, Fifield K, Vasconcelos P. 2005. Terrestrial chlorine-36 production from spallation of iron. *Abstract of the 10th International Conference on Accelerator Mass Spectrometry*. September 5–10, 2005, Berkeley, USA. [<http://lnl.confex.com/lnl/ams10/techprogram/P1397.HTM>]
- Stone JO, Allan GL, Fifield LK, et al. 1996. Cosmogenic  $^{36}\text{Cl}$  from calcium spallation. *Geochimica et Cosmochimica Acta* **60**: 679–692.
- Swanson TW, Caffee ML., 2001. Determination of  $^{36}\text{Cl}$  production rates derived from the well-dated deglaciation surfaces of Whidbey and Fidalgo Islands, Washington. *Quaternary Research* **56**: 366–382.
- Zreda MG, Phillips FM, Elmore D, et al. 1991. Cosmogenic chlorine-36 production rates in terrestrial rocks. *Earth and Planetary Sciences Letters* **105**: 94–109.